Proximity potential and temperature effects on α-decay half-lives

A. Daei-Ataollah,* O. N. Ghodsi, and M. Mahdavi
Department of Physics, School of Sciences, University of Mazandaran, Post Office Box 47415-416, Babolsar, Iran

(Received 9 July 2017; revised manuscript received 6 March 2018; published 31 May 2018)

In order to calculate the α-decay half-lives of a wide range of heavy and superheavy nuclei, we introduced a modified temperature-dependent surface energy coefficient in the proximity potential based on thermal properties of liquids and hot nuclei. An increase in the α-decay half-life was observed by decreasing the surface energy coefficient as a result of temperature incorporation of the parent nuclei. The introduced temperature-dependent surface energy coefficient evaluated the half-lives which were in good agreement with the experimental data. Moreover, the results of the present paper confirm the closed-shell effects.

DOI: 10.1103/PhysRevC.97.054621

I. INTRODUCTION

The study of α decay provides a reliable way to discover new nuclei and elements via decay chains [1–6]. Furthermore, its study provides extensive knowledge on nuclear structure and properties of exotic nuclei in drip-line, closed-shell, and superheavy regions [7–12]. Valuable information on ground-state energy, ground-state half-life, nuclear spin and parity, magic numbers, island of stability, isomeric states, nuclear deformation, nuclear clustering, and effective interaction are the important issues of α-decay studies [13–19]. As a powerful tool, α-decay investigation can therefore extend our conception of nuclei. On the experimental side, α decay benefits from highly efficient detection with high resolution and low background [20–27].

A proximity formalism based on intrinsic properties of the nuclei, such as surface energy, thickness, and nuclei radii was introduced in fusion reactions [28]. The effect of physical concepts, such as spin, isospin, closed shells, fine structure, deformation, and orientation are investigated in a proximity formalism [29–35]. Although various versions of the proximity formalism have been formulated for fusion studies, only a few have been applied or modified for α-decay studies. The model proposed by Dutt [36] is one of the latest and applicable versions of the proximity potential obtained through recent knowledge of the universal function and surface energy coefficient for fusion reactions. Our study revealed that this model offers satisfactory results for α-decay studies [37]. Although Dutt's model [36], similar to most other proximity potentials, shows good performance for even-even nuclei, the results were not so satisfying for odd-A and odd-odd nuclei. In order to reduce these discrepancies, this study examines α emitters by integrating temperature effects on the surface energy coefficient of the proximity formalism.

As the α-decay process is a quantum tunneling effect through a potential barrier, the height and position of the barrier as well as its shape play a crucial role in the calculation of α-decay half-lives. The surface energy coefficient has a considerable effect on the potential barrier. Over time, with the progress in theoretical models as well as experimental instruments and methods, many modifications have been applied to the surface energy coefficient to obtain the proximity potential that can lead to agreement with experimental data (see Ref. [37] and references therein). These changes include modified sets of the surface energy and asymmetry constants (γ_0,k_s). The adjustment of the surface energy constant causes changes in barrier characteristics. A larger γ gives a more attractive and stronger nuclear potential, which leads to barrier lowering and pocket deepening [35,38,39].

From an experimental perspective, different methods have been proposed to measure nuclear temperatures. They can be categorized into three main groups: population, kinetic, and thermal-energy approaches. On the theoretical side, a large number of studies has obtained the nuclear equation of state and calculated critical temperature of semi-infinite nuclear matter. (See Ref. [40] and references therein.) Temperature dependence has been applied to potential and effective mass parameters, such as radius, diffuseness, and surface tension [41–43].

Including temperature dependence in the proximity models can affect the results in two ways: (1) in the effective sharp radius and the surface width [32,35,44] and (2) in the surface energy coefficient. This difficulty can be managed in two different ways: starting from a fundamental approach free from adjustable parameters and adjusting different parameters of the model to known experimental data.

In the current research, we employ the formulas used to study the thermal behavior of liquids and hot nuclei in order to modify the surface energy coefficient in the proximity formalism. To optimize the suggested surface energy coefficient in studying the α-decay process, the variables of this temperature-dependent (TD) formula are adjusted such that the calculated α-decay half-lives for a wide range of α emitters are in agreement with those reported experimentally.

This paper is organized as follows: Formalisms employed to calculate the α-decay half-life, the interaction potential, and the

*aysan.daei@gmail.com

temperature dependence of the proximity potential are given in Sec. II. The results and discussion are presented in Sec. III, and finally, concluding remarks are given in Sec. IV.

II. THEORETICAL FRAMEWORK

A. Description of the α-decay half-life formalism

The decay half-life of a parent nucleus (A,Z) to an α particle (A_α,Z_α) and a daughter nucleus (A_d,Z_d) is calculated using

$$T_{1/2} = \frac{\ln 2}{\lambda} = \frac{\ln 2}{\nu P_\alpha}, \tag{1}$$

where λ is the decay constant and ν represents the assault frequency thus,

$$\nu = \frac{\omega}{2\pi} = \frac{2E_\nu}{h}. \tag{2}$$

The correlation between the zero-point vibration energy E_ν and the released energy of the emitted α-particle Q_α is expressed using the empirical formula [45] thus,

$$E_\nu = \begin{cases} 0.1045Q_\alpha & \text{for even } Z\text{-even } N \text{ parent nuclei,} \\ 0.0962Q_\alpha & \text{for odd } Z\text{-even } N \text{ parent nuclei,} \\ 0.0907Q_\alpha & \text{for even } Z\text{-odd } N \text{ parent nuclei,} \\ 0.0767Q_\alpha & \text{for odd } Z\text{-odd } N \text{ parent nuclei.} \end{cases} \tag{3}$$

Based on the one-dimensional Wentzel-Kramers-Brillouin (WKB) semiclassical approximation, the α-decay penetration probability P_α through the potential barrier is calculated as

$$P_\alpha = \exp\left(\frac{-2}{\hbar}\int_{R_a}^{R_b}\sqrt{2\mu[V_T(r)-Q_\alpha]}dr\right), \tag{4}$$

where μ is the reduced mass of the α-daughter system. The inner and outer classical turning points R_a and R_b respectively, are calculated as

$$V_T(R_a) = Q_\alpha = V_T(R_b). \tag{5}$$

B. Description of the potential formalism

Total interaction potential $V_T(r)$ between the α particle and the daughter nucleus is composed of three main parts: the repulsive Coulomb potential $V_C(r)$, the attractive nuclear potential $V_N(r)$, and the centrifugal potential $V_l(r)$,

$$V_T(r) = V_N(r) + V_C(r) + V_l(r). \tag{6}$$

Using the pointlike plus uniform model, the Coulomb potential $V_C(r)$ is defined as

$$V_C(r) = Z_a Z_d e^2 \begin{cases} \frac{1}{r} & \text{for } r \geqslant R_c, \\ \frac{1}{2R_c}\left[3-\left(\frac{r}{R_c}\right)^2\right] & \text{for } r \leqslant R_c, \end{cases} \tag{7}$$

where r is the distance between the fragment centers and R_c is the touching radial separation between the α particle and the daughter nucleus.

The l-dependent centrifugal potential $V_l(r)$ is as follows:

$$V_l(r) = \hbar^2\frac{l(l+1)}{2\mu r^2}, \tag{8}$$

where l is the orbital angular momentum carried away by the emitted α particle.

The proximity formalism can be used to calculate the nuclear potential $V_N(r)$ between the α particle and the daughter nucleus [28] thus,

$$V_N(r) = 4\pi\gamma b\bar{R}\Phi(\xi). \tag{9}$$

This potential is related to the geometry and shape of the participant nuclei and universal function $(\Phi(\xi))$.

The surface energy coefficient γ based on Ref. [46] is given as

$$\gamma = \gamma_0\left[1-k_s A_s^2\right]\ \text{MeV/fm}^2, \tag{10}$$

where $A_s = \frac{N-Z}{A}$ represents the neutron/proton excess. γ_0 and k_s are the surface energy constant and the surface asymmetry constant, respectively. The original set of these constants based on Myers and Świątecki's work [46] was introduced as $\gamma_0 = 1.01734\ \text{MeV/fm}^2$ and $k_s = 1.79$. In the present paper, the modified set of these constants $\gamma_0 = 1.25284\ \text{MeV/fm}^2$ and $k_s = 2.345$, denoted as γ-MN 1995 [47] was used. b is the surface width ($b \approx 1$ fm) and $\bar{R}$ denotes the reduced radius as

$$\bar{R} = \frac{C_1C_2}{C_1+C_2}, \tag{11}$$

where C_i is the matter radius (Süssmann's central radius). The index $i = 1,2$ refers to the α particle and daughter nucleus, respectively. Based on the droplet model, Myers and Świątecki expressed C_i in terms of half-density radius c_i as [48]

$$C_i = c_i + \left(\frac{N_i}{a_i}\right)t_i \quad (i = 1,2), \tag{12}$$

where the neutron skin of nucleus t derives the form

$$t_i = \frac{3}{2}r_0\left(\frac{JI_i - \frac{1}{12}c_1Z_iA_i^{-1/3}}{Q+\frac{9}{4}JA_i^{-1/3}}\right) \quad (i = 1,2), \tag{13}$$

in which the radius constant $r_0 = 1.14$ fm, the symmetry energy coefficient $J = 32.65$ MeV, $I = (N-Z)/A$, $c_i = 3e^2/5r_0 = 0.757895$ MeV, and the neutron skin stiffness coefficient $Q = 35.4$ MeV.

The half-density radius of the charge distribution in terms of nuclear charge radius R_{00} is expressed as [48]

$$c_i = R_{ooi}\left(1-\frac{7}{2}\frac{b^2}{R_{ooi}^2}-\frac{49}{8}\frac{b^4}{R_{ooi}^4}+\cdots\right) \quad (i = 1,2). \tag{14}$$

By fitting the measured root-mean-square values of the charge distribution $\langle r^2\rangle^{1/2}$, the charge radius formula was determined as [36]

$$R_{ooi} = 1.171A_i^{1/3} + 1.427A_i^{-1/3} \quad (i = 1,2). \tag{15}$$

The model is based on the fact that the diffuseness of the nuclei is much smaller than their radii.

The modified parametrization of the universal function $\Phi(\xi)$ was given as [49]

$$\Phi(\xi) = \begin{cases} -1.7817 + 0.9270\xi + 0.143\xi^2 - 0.09\xi^3 & \text{for } \xi \leqslant 0.0, \\ -1.7817 + 0.9270\xi + 0.01696\xi^2 - 0.5148\xi^3 & \text{for } 0.0 \leqslant \xi \leqslant 1.9475, \\ -4.41\exp\left(\frac{-\xi}{0.7176}\right) & \text{for } \xi \geqslant 1.9475, \end{cases} \tag{16}$$

where $\xi = s/b$ is the minimum separation distance in units of the surface width and s refers to the separation distance between the half-density surfaces of the fragments,

$$s = r - C_1 - C_2 \text{ fm}. \tag{17}$$

This model is referred to as Dutt 2011. A detailed investigation of over 395 reactions [36] and our comparative study of over 344 α decays [37] revealed the suitability of this model for both fusion and α-decay studies.

C. Temperature dependence of the proximity potential

To advance the proximity nuclear potential, the temperature dependence of the potential can be applied on the surface energy coefficient. It is known that surface tension of liquids γ is dependent on temperature T. The T dependence is such that surface tension decreases with an increase in temperature vanishing at a so-called critical temperature T_c. The simple and widely used Guggenheim-Katayama–van der Waals empirical equation for the T dependence of surface tension is given by [50–54]:

$$\gamma = \gamma(T=0)\left(1 - \frac{T}{T_c}\right)^n \text{ mN/m or mJ/m}^2, \tag{18}$$

where $\gamma(T=0)$ is a system-dependent constant being the surface tension at absolute zero and n is an empirically fitted exponent which is determined by comparison with surface tension experimental data.

Like the temperature dependence of surface tension of liquids, such a dependence also exists for nuclei. Jaqaman [55] using a finite-temperature generalized liquid-drop model derived the temperature dependence of the surface tension of a hot nucleus as

$$\gamma(T) = 1.14\left(1 - \frac{T}{T_c}\right)^2 \text{ MeV/fm}^2. \tag{19}$$

This relation was obtained by generalizing the equation of state for the asymmetric nuclear matter using the Skyrme-type effective interaction.

With consistent temperature dependence of the surface energy coefficient for liquids and hot nuclei and in contrast with experimental α-decay half-lives, we explored the temperature dependence of the surface energy coefficient in the proximity formalism by using the following relation:

$$\gamma(T) = \gamma(T=0)(1 - pT)^q \text{ MeV/fm}^2, \tag{20}$$

where p and q are two constants obtained by fitting to the experimentally measured α-decay half-lives of a wide range of nuclei. $\gamma(T=0)$ refers to the temperature-independent (T-IND) surface energy coefficient as calculated using Eq. (10).

The nuclear temperature T (in units of MeV) is correlated to the excitation energy of the compound nucleus E^*_{CN} as [56]

$$E^*_{CN} = E_\alpha + Q_\alpha = \frac{1}{a}AT^2 - T \text{ (MeV)}, \tag{21}$$

where E_α represents the kinetic energy of the α particle and $a \cong$ 9 or 10 MeV for intermediate-mass or superheavy systems, respectively.

III. RESULTS AND DISCUSSION

In our previous work [37], we studied the α-decay half-lives of 344 isotopes of nuclei within 28 versions of the proximity potential model in the framework of the WKB approximation. The proximity model denoted as Dutt 2011 is one of the best proximity versions to predict α-decay half-lives with the least deviations with respect to the experimental values. Consequently, in this research, it was applied to investigate temperature effects. Although the results from Dutt 2011 were in good agreement with experimental half-lives, deviations were not negligible for odd-A and odd-odd nuclei. In this paper, we studied α emitters by considering temperature dependence in the nuclear surface energy constant using Eq. (20). The coefficients p and q in this equation were adapted by an adjustment to the experimental data of α-decay half-lives. This potential was reported using the TD prefix (i.e., TD-Dutt 2011). The ranges of the atomic and mass numbers of chosen parent nuclei with definite experimental α-decay half-lives were $80 \leqslant Z \leqslant 102$ and $176 \leqslant A \leqslant 257$, respectively.

The calculated temperatures of all parent nuclei using Eq. (21) versus the mass numbers of parent nuclei are shown

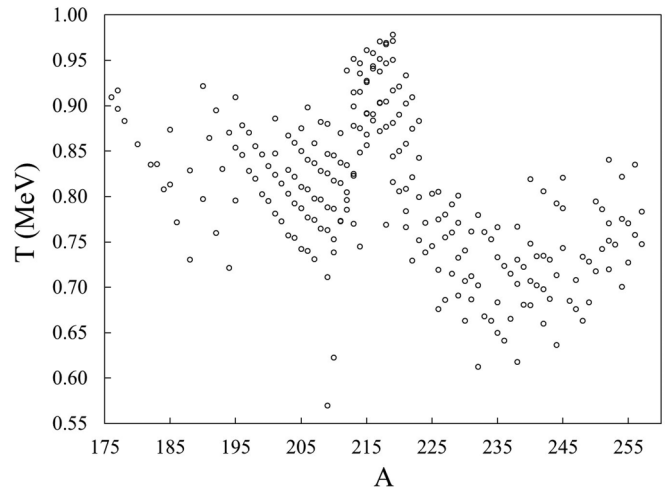

FIG. 1. The calculated temperatures [Eq. (21)] of the parent nuclei with $80 \leqslant Z \leqslant 102$ during the α-decay process as a function of mass number of the parent nuclei.

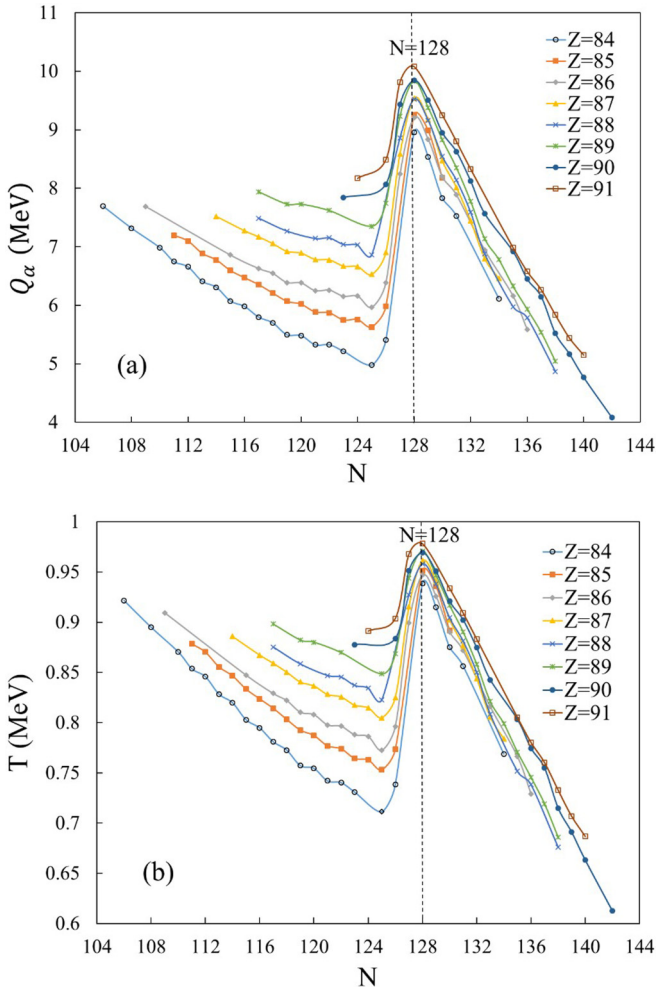

FIG. 2. Variation of (a) released energy of an emitted α particle and (b) temperature of the parent nuclei versus the neutron number of the parent isotopic systems with $84 \leqslant Z \leqslant 91$.

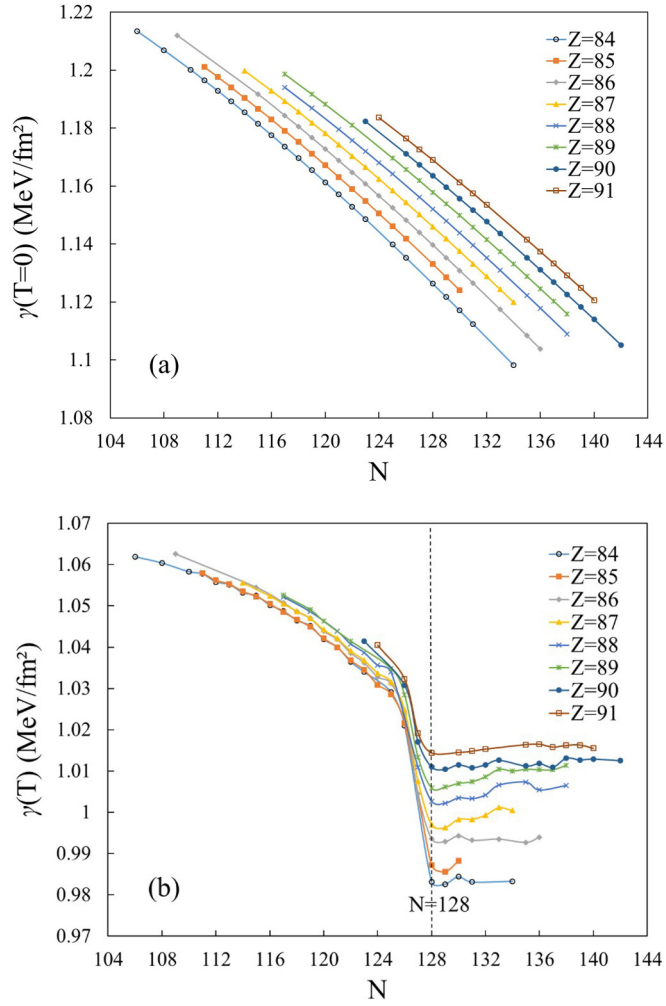

FIG. 3. (a) T-IND surface energy coefficient $\gamma(T = 0)$ and (b) TD surface energy coefficient $\gamma(T)$ versus the neutron number of the parent isotopic systems with $84 \leqslant Z \leqslant 91$.

in Fig. 1. The values of Q_α are the same as those in Ref. [57]. This paper shows that the temperature values of parent nuclei were in the range of 0.55–1.0 MeV.

The variation of energy released from the emitted α particle (Q_α) and temperature of parent nuclei T versus the neutron number of parent nuclei can be seen in Figs. 2(a) and 2(b), respectively, for isotopic groups of parent nuclei with $84 \leqslant Z \leqslant 91$. The results also show that, for each isotonic group, a parent nucleus with a bigger atomic number emits more energetic α particles. It is also shown that, for each isotopic group, the highest Q_α and the highest T belong to the $N = 128$ isotope, which leads to a closed-shell daughter nucleus with the neutron magic number $N_d = 126$.

Using the proximity potential within the WKB approximation, the α-decay half-lives of parent nuclei were calculated using Eq. (1). The half-lives were calculated with respect to two concepts: (1) the T-IND proximity potential and (2) the proximity potential with the TD surface energy coefficient.

In order to determine the coefficients p and q in Eq. (20), the symmetric mean absolute percentage error (SMAPE) of the decimal logarithm of α-decay half-lives was employed thus,

$$\mathrm{SMAPE} = \frac{1}{n}\sum_{i=1}^{n}\left(\frac{\left|\log_{10}\left(T_{1/2}^{\mathrm{cal}}\right)_i - \log_{10}\left(T_{1/2}^{\mathrm{exp}}\right)_i\right|}{\log_{10}\left(T_{1/2}^{\mathrm{cal}}\right)_i + \log_{10}\left(T_{1/2}^{\mathrm{exp}}\right)_i}\right) \times 100, \tag{22}$$

where parameter n refers to the number of nuclei under consideration and $\log_{10}(T_{1/2}^{\mathrm{exp}})$ and $\log_{10}(T_{1/2}^{\mathrm{cal}})$ are the experimental and calculated data for the decimal logarithm of α-decay half-lives, respectively. The experimental data for α-decay half-lives were obtained from Refs. [58–60].

By comparing the experimental α-decay half-lives and minimizing SMAPE, we estimated coefficients p and q in Eq. (20) to be 0.07 and 2, respectively, for all categories of even-even, even-odd, odd-even, and odd-odd parent nuclei. Therefore the temperature dependence of the surface energy constant is expressed as

$$\gamma(T) = \gamma(T = 0)(1 - 0.07T)^2 \ \mathrm{MeV/fm^2}. \tag{23}$$

Figures 3(a) and 3(b) show the T-IND surface energy coefficient $\gamma(T = 0)$ and TD surface energy coefficient $\gamma(T)$

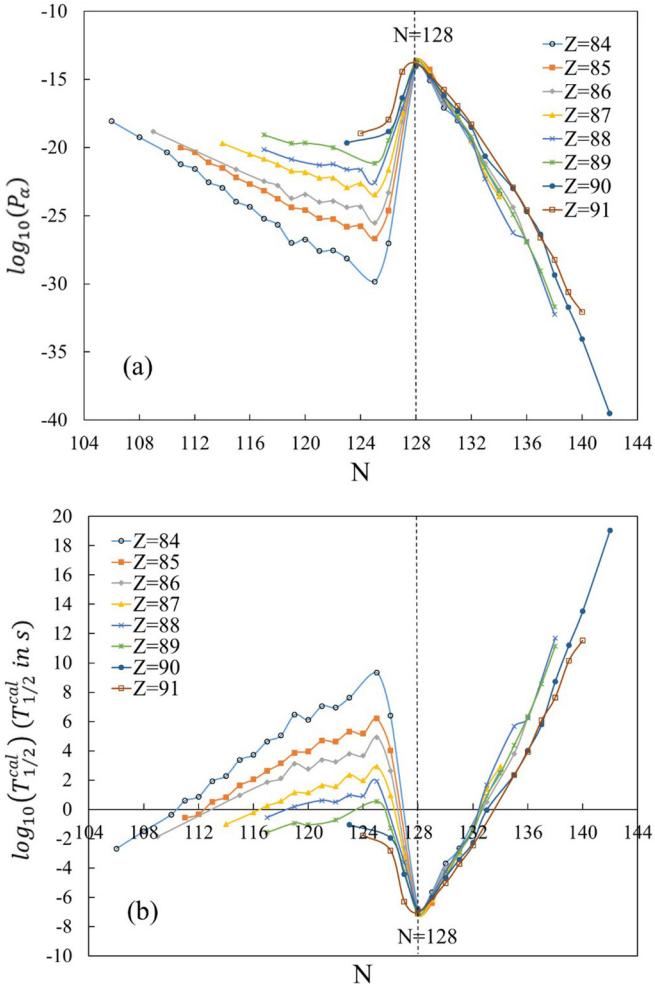

FIG. 4. Variation of (a) penetration probability of the α particle on the decimal logarithmic scale and (b) the decimal logarithm of the α-decay half-lives with the neutron number of the parent nuclei predicted by the TD-Dutt 2011 model for isotopic systems of $84 \leqslant Z \leqslant 91$.

calculated using Eqs. (10) and (23), respectively. The isotopic chains are similar to those of Fig. 2. By increasing Z from 84 to 91, $\gamma(T = 0)$ and $\gamma(T)$ showed a corresponding increase. It was also shown that $\gamma(T = 0)$ exhibited a decreasing linear trend with increasing N, whereas the modified surface energy coefficient $\gamma(T)$ had a valley around $N = 128$ which points out the closed-shell effects.

The decimal logarithm of the penetration probability of α through the potential barrier $\log_{10}(P_\alpha)$ and the decimal logarithm of the α-decay half-lives $\log_{10}(T^{\rm cal}_{1/2})$ calculated using TD-Dutt 2011 are shown in Figs. 4(a) and 4(b), respectively. For the parent nuclei with two neutrons outside the closed shell, the α particle penetrated more easily than other isotopes. Shell closure has a major effect on the α-decay half-life as $\log_{10}(T^{\rm cal}_{1/2})$ reaches the lowest amount around $N = 128$, thus confirming the higher instability of the parent nucleus that decays in the closed-shell daughter nucleus. Additionally, it is apparent that, for each isotonic group, the parent nucleus with the largest Z had the shortest $\log_{10}(T^{\rm cal}_{1/2})$.

The calculated half-lives were compared with the results of the l-dependent empirical formulas derived by Royer for α-decay half-lives $\log_{10}(T_{1/2}) = f(Q_\alpha, l, A, Z)$ [61] and with those of the unified model for α decay and α capture (UMADAC) [59].

The calculated SMAPEs with respect to the total, even-even, even-odd, odd-even, and odd-odd α emitters for T-IND Dutt 2011, TD-Dutt 2011, Royer's empirical formula [61], and UMADAC are shown in Table I. All investigations used a total of 240 emitters consisting of 81 even-even, 61 even-odd, 60 odd-even, and 38 odd-odd α emitters.

Table I shows that by including the present temperature dependence in the proximity model the total SMAPE was improved by more than 50%. In addition, the results produced by the TD model were comparable with those of the other approaches mentioned.

IV. CONCLUSION

The α-decay half-lives of nuclei with atomic numbers $80 \leqslant Z \leqslant 102$ and mass numbers $176 \leqslant A \leqslant 257$ were evaluated based on the WKB penetration probability. The proximity model denoted as Dutt 2011 was used to determine the nuclear part of the potential. To improve the calculated α-decay half-lives, a temperature-dependent surface energy coefficient was applied to the proximity potential. A unified TD formula was presented for all even-even, even-odd, odd-even, and odd-odd nuclei. The theoretical results were compared with experimental data, l-dependent empirical formulas of the half-life, and UMADAC. By incorporating the temperature dependence of the surface energy coefficient, a considerable improvement in the α-decay half-lives was obtained. Furthermore, the results of TD-Dutt 2011 established the shell closure effects on α-decay released energy, the temperature of the parent nucleus, the surface energy coefficient, the penetration probability, and the α-decay half-life. Our results also showed that, for each isotopic family, the peak temperature and valley of the half-life belonged to a parent nucleus that decayed to a daughter nucleus with a neutron magic number.

TABLE I. Comparison of SMAPEs (percentage) of the decimal logarithm of the α-decay half-lives for a full set of nuclei derived using different approaches. All investigations employ 240 total, 81even-even, 61 even-odd, 60 odd-even, and 38 odd-odd α emitters.

Model	Total	Even-even	Even-odd	Odd-even	Odd-odd	Reference
T-IND Dutt 2011	6.44	3.59	9.66	4.35	10.61	Present paper
TD-Dutt 2011	2.71	2.41	2.57	2.99	3.13	Present paper
Royer: l dependent	3.69	2.31	7.58	3.20	1.14	[61]
Denisov: UMADAC	3.39	1.57	7.31	2.55	2.32	[59]

[1] S. Hofmann and G. Münzenberg, Rev. Mod. Phys. **72**, 733 (2000).
[2] T. N. Ginter, K. E. Gregorich, W. Loveland, D. M. Lee, U. W. Kirbach, R. Sudowe, C. M. Folden III, J. B. Patin, N. Seward, P. A. Wilk, P. M. Zielinski, K. Aleklett, R. Eichler, H. Nitsche, and D. C. Hoffman, Phys. Rev. C **67**, 064609 (2003).
[3] V. Y. Denisov and A. A. Khudenko, Phys. Rev. C **81**, 034613 (2010).
[4] S. B. Duarte and N. Teruya, Phys. Rev. C **85**, 017601 (2012).
[5] Y. T. Oganessian, V. K. Utyonkov, F. S. Abdullin, S. N. Dmitriev, R. Graeger, R. A. Henderson, M. G. Itkis, Y. V. Lobanov, A. N. Mezentsev, K. J. Moody, S. L. Nelson, A. N. Polyakov, M. A. Ryabinin, R. N. Sagaidak, D. A. Shaughnessy, I. V. Shirokovsky, M. A. Stoyer, N. J. Stoyer, V. G. Subbotin, K. Subotic, A. M. Sukhov, Y. S. Tsyganov, A. Türler, A. A. Voinov, G. K. Vostokin, P. A. Wilk, and A. Yakushev, Phys. Rev. C **87**, 034605 (2013).
[6] C. Xu, X. Zhang, and Z. Ren, Nucl. Phys. A **898**, 24 (2013).
[7] M. Freer, E. Casarejos, L. Achouri, C. Angulo, N. I. Ashwood, N. Curtis, P. Demaret, C. Harlin, B. Laurent, M. Milin, N. A. Orr, D. Price, R. Raabe, N. Soić, and V. A. Ziman, Phys. Rev. Lett. **96**, 042501 (2006).
[8] D. Seweryniak, K. Starosta, C. N. Davids, S. Gros, A. A. Hecht, N. Hoteling, T. L. Khoo, K. Lagergren, G. Lotay, D. Peterson, A. Robinson, C. Vaman, W. B. Walters, P. J. Woods, and S. Zhu, Phys. Rev. C **73**, 061301 (2006).
[9] M. Ismail, A. Y. Ellithi, M. M. Botros, and A. Adel, Phys. Rev. C **81**, 024602 (2010).
[10] Y. Z. Wang, J. M. Dong, B. B. Peng, and H. F. Zhang, Phys. Rev. C **81**, 067301 (2010).
[11] Y. Qian and Z. Ren, Nucl. Phys. A **852**, 82 (2011).
[12] Y. Qian, Z. Ren, and D. Ni, Nucl. Phys. A **866**, 1 (2011).
[13] R. Zhong-zhou and X. Gong-ou, Phys. Rev. C **36**, 456 (1987).
[14] H. Horiuchi, Nucl. Phys. A **522**, 257 (1991).
[15] J. Wauters, N. Bijnens, P. Dendooven, M. Huyse, H. Y. Hwang, G. Reusen, J. von Schwarzenberg, P. Van Duppen, R. Kirchner, and E. Roeckl, Phys. Rev. Lett. **72**, 1329 (1994).
[16] P. E. Hodgeson and E. Betak, Phys. Rep. **374**, 1 (2003).
[17] H. F. Zhang, Y. Gao, N. Wang, J. Q. Li, E. G. Zhao, and G. Royer, Phys. Rev. C **85**, 014325 (2012).
[18] D. S. Delion, S. Peltonen, and J. Suhonen, Phys. Rev. C **73**, 014315 (2006).
[19] A. P. Leppänen, J. Uusitalo, M. Leino, S. Eeckhaudt, T. Grahn, P. T. Greenlees, P. Jones, R. Julin, S. Juutinen, H. Kettunen, P. Kuusiniemi, P. Nieminen, J. Pakarinen, P. Rahkila, C. Scholey, and G. Sletten, Phys. Rev. C **75**, 054307 (2007).
[20] I. Ahmad and J. L. Lerner, Nucl. Phys. A **413**, 423 (1984).
[21] A. Becerril-Vilchis, A. Cortés, F. Dayras, and J. de Sanoit, Nucl. Instrum. Methods Phys. Res., Sect. A **369**, 613 (1996).
[22] F. Dayras and N. Chauvin, Nucl. Instrum. Methods Phys. Res., Sect. A **530**, 391 (2004).
[23] E. García-Toraño, M. T. Crespo, M. Roteta, G. Sibbens, S. Pommé, A. M. Sáchez, M. P. Rubio Montero, S. Woods, and A. Pearce, Nucl. Instrum. Methods Phys. Res., Sect. A **550**, 581 (2005).
[24] P. Belli, R. Bernabei, F. Cappella, R. Cerulli, C. J. Dai, F. A. Danevich, A. d'Angelo, A. Incicchitti, V. V. Kobychev, S. S. Nagorny, S. Nisi, F. Nozzoli, D. Prosperi, V. I. Tretyak, and S. S. Yurchenko, Nucl. Phys. A **789**, 15 (2007).
[25] Y. S. Jang, G. B. Kim, K. J. Kim, M. S. Kim, H. J. Lee, J. S. Lee, K. B. Lee, M. K. Lee, S. J. Lee, H. C. Ri, W. S. Yoon, Y. N. Yuryev, and Y. H. Kim, Appl. Radiat. Isot. **70**, 2255 (2012).
[26] M. Marouli, S. Pommé, V. Jobbágy, R. Van Ammel, J. Paepen, H. Stroh, and L. Benedik, Appl. Radiat. Isot. **87**, 292 (2014).
[27] S. Pommé, E. García-Toraño, M. Marouli, M. T. Crespo, V. Jobbágy, R. Van Ammel, J. Paepen, and H. Stroh, Appl. Radiat. Isot. **87**, 315 (2014).
[28] J. Blocki, J. Randrup, W. J. Świątecki, and C. F. Tsang, Ann. Phys. (NY) **105**, 427 (1977).
[29] K. P. Santhosh, J. G. Joseph, and S. Sahadevan, Phys. Rev. C **82**, 064605 (2010).
[30] K. P. Santhosh and B. Priyanka, Eur. Phys. J. A **49**, 150 (2013).
[31] K. P. Santhosh, J. G. Joseph, B. Priyanka, and S. Sahadevan, J. Phys. G: Nucl. Part. Phys. **38**, 075101 (2011).
[32] R. K. Gupta, N. Singh, and M. Manhas, Phys. Rev. C **70**, 034608 (2004).
[33] M. Bansal, S. Chopra, R. K. Gupta, R. Kumar, and M. K. Sharma, Phys. Rev. C **86**, 034604 (2012).
[34] N. S. Rajeswari and M. Balasubramaniam, J. Phys. G: Nucl. Part. Phys. **40**, 035104 (2013).
[35] R. Kumar, Phys. Rev. C **84**, 044613 (2011).
[36] I. Dutt, Pramana **76**, 921 (2011).
[37] O. N. Ghodsi and A. Daei-Ataollah, Phys. Rev. C **93**, 024612 (2016).
[38] I. Dutt and R. K. Puri, Phys. Rev. C **81**, 064609 (2010).
[39] I. Dutt and R. K. Puri, Phys. Rev. C **81**, 047601 (2010).
[40] A. Kelić, J. B. Natowitz, and K. H. Schmidt, Eur. Phys. J. A **30**, 203 (2006).
[41] G. Sauer, H. Chandra, and U. Mosel, Nucl. Phys. A **264**, 221 (1976).
[42] S. Shlomo and J. B. Natowitz, Phys. Rev. C **44**, 2878 (1991).
[43] G. Royer and J. Mignen, J. Phys. G: Nucl. Part. Phys. **18**, 1781 (1992).
[44] R. K. Gupta, D. Singh, R. Kumar, and W. Greiner, J. Phys. G: Nucl. Part. Phys. **36**, 075104 (2009).
[45] D. N. Poenaru, W. Greiner, M. Ivaşcu, D. Mazilu, and I. H. Plonski, Z. Phys. A: At. Nucl. **325**, 435 (1986).
[46] W. D. Myers and W. J. Świątecki, Nucl. Phys. **81**, 1 (1966).
[47] P. Möller, J. R. Nix, W. D. Myers, and W. J. Świątecki, At. Data Nucl. Data Tables **59**, 185 (1995).
[48] W. D. Myers and W. J. Świątecki, Phys. Rev. C **62**, 044610 (2000).
[49] J. Blocki and W. J. Świątecki, Ann. Phys. (NY) **132**, 53 (1981).
[50] N. K. Adam, *The Physics and Chemistry of Surfaces*, 3rd ed. (Oxford University Press, London, 1941).
[51] E. A. Guggenheim, J. Chem. Phys. **13**, 253 (1945).
[52] P. G. de Gennes, F. Brochard-Wyart, and D. Quere, *Capillarity and Wetting Phenomena: Drops, Bubbles, Pearls, Waves*, translated from French by A. Reisinger (Springer-Verlag, New York, 2004).
[53] P. O. Biney, W. G. Dong, and J. H. Lienhard, J. Heat Transfer **108**, 405 (1986).
[54] A. P. Fröba, S. Will, and A. Leipertz, Int. J. Thermophys. **21**, 1225 (2000).
[55] H. R. Jaqaman, Phys. Rev. C **40**, 1677 (1989).
[56] K. J. Le Couteur and D. W. Lang, Nucl. Phys. **13**, 32 (1959).
[57] M. Wang, G. Audi, A. H. Wapstra, F. G. Kondev, M. MacCormick, X. Xu, and B. Pfeiffer, Chin. Phys. C **36**, 1603 (2012).
[58] D. N. Basu, Phys. Lett. B **566**, 90 (2003).
[59] V. Y. Denisov and A. A. Khudenko, At. Data Nucl. Data Tables **95**, 815 (2009).
[60] G. Audi, F. G. Kondev, M. Wang, B. Pfeiffer, X. Sun, J. Blachot, and M. MacCormick, Chin. Phys. C **36**, 1157 (2012).
[61] G. Royer, Nucl. Phys. A **848**, 279 (2010).